VOL. 6, NO. 1, JAN.-MARCH 1992 J. THERMOPHYSICS 27

Numerical Simulation of Rarefied Gas Flow Through a Slit

Chan-Hong Chung,[*] Duen-Ren Jeng,[†] Kenneth J. De Witt,[‡] and Theo G. Keith Jr.[§]
University of Toledo, Toledo, Ohio 43606

Two different approaches, the finite-difference method coupled with the discrete-ordinate method (FDDO), and the direct-simulation Monte-Carlo (DSMC) method, are used in the analysis of the flow of a rarefied gas from one reservoir to another through a two-dimensional slit. The cases considered are for a vacuum downstream, finite pressure ratios, and isobaric conditions with thermal diffusion, which are not well established in spite of the simplicity of the flow field. In the FDDO analysis, by employing the discrete-ordinate method, the Boltzmann equation simplified by a model collision integral is transformed to a set of partial differential equations that are continuous in physical space but are point functions in molecular velocity space. The set of partial differential equations are solved by means of a finite-difference approximation. In the DSMC analysis, the variable hard sphere (VHS) model is used as a molecular model and the no time counter (NTC) method is employed as a collision sampling technique. The results of both the FDDO and the DSMC methods show good agreement. The FDDO method requires less computational effort than the DSMC method by a factor of 4 in CPU memory size and by factors of 10 to 40 in CPU time, depending on the degree of gas rarefaction.

Nomenclature

A_c = collision frequency
b = density ratio between two reservoirs
$\mathbf{C}$ = peculiar velocity, $\mathbf{V} - \mathbf{U}$
C_r = collision relative speed
d = characteristic length of flow field
f = number density distribution function, $f(x, y, V_x, V_y, V_z)$
g, h = reduced distribution functions
J_t = Jacobian of transformation
Kn = Knudsen number
m = mass of a molecule
N = order of quadrature
N_m = number of molecules in a cell
n = number density
$\mathbf{n}$ = inward normal vector to surface
n_w = wall number flux
P = pressure
Pr = Prandtl number
P_δ = weighting factor of quadrature
Q = total flux
Q_0 = theoretical free-molecular total flux
Q_x = flux
Q_{x0} = theoretical free-molecular flux
$\mathbf{q}$ = heat flux vector
R = gas constant
s = viscosity-temperature exponent
T = temperature
$\mathbf{U}$ = macroscopic flow velocity vector
V = speed of molecule
$\mathbf{V}$ = velocity of molecule
V_0 = most probable thermal speed, $\sqrt{2RT_0}$
V_x, V_y, V_z = velocity components of molecule in Cartesian coordinates
V_δ = discrete velocity point
w = exponent of variable hard sphere model
x, y, z = Cartesian coordinates of physical space
Y_0 = slit half width
η, ξ = coordinates in transformed physical space
λ = molecular mean free path
μ = viscosity
σ_T = collision cross section
ϕ = angle in transformed velocity space

Subscripts and Caps
b = downstream reservoir condition
o = upstream reservoir condition
δ = discrete ordinate point, ($\delta = 1, 2, \ldots, N\text{-}1, N$)
$\wedge$ = dimensionless variable

Introduction

THE flow of a rarefied gas from one reservoir to another through a channel is induced by either a pressure difference, a temperature difference, or a combination of the two. Applications of this type of flow are found in vacuum science, molecular beam technology, and high altitude flight such as the flow field for low-thrust resistojets. Many investigations have been reported for simple geometries such as a slit, an orifice, a two-dimensional slot, and a circular tube. Most of these studies are confined to the flow induced by a pressure difference only.

The problem of the flow through a slit or an orifice has been given much attention. Liepmann[1] pointed out that this problem offers the possibility of a comparison between experiment and a kinetic theory analysis which is not sensitive to the nature of molecular interaction with the boundary surfaces. Liepmann was the first to analyze both theoretically and experimentally the mass flow rate of a rarefied gas through an orifice into a vacuum reservoir. In his investigation, the reservoirs are at the same temperature and the upstream reservoir pressure is in the range of continuum to free-molecular flow conditions. Narasimha[2] obtained an expression for the average mass flow rate based on the centerline value for a circular orifice by using Willis'[3] iterative method. In this method, the Bhatnagar-Gross-Krook (BGK)[4] model equation is converted to an integral form and iterations are performed on it starting from the free-molecular solution for the distribution function. Willis[5] improved Narasimha's method by numerically evaluating the quadratures in the integral equation for the flux obtained from the BGK model and removing the

---

Presented as Paper 90-1694 at the AIAA/ASME 5th Joint Thermophysics and Heat Transfer Conference, Seattle, WA, June 18–20, 1990; received July 20, 1990; revision received Dec. 26, 1990; accepted for publication Dec. 27, 1990.

[*] Research Associate, Chemical Engineering Department. Member AIAA.

[†] Professor, Mechanical Engineering Department.

[‡] Professor, Chemical Engineering Department.

[§] Professor, Mechanical Engineering Department. Associate Fellow AIAA.

simplifying assumptions which were used by Narasimha. He calculated the total as well as the local mass flow rate of a nearly free-molecular flow through a slit as well as for an orifice by performing one iteration on the integral equation for the flux. In his method, however, the effect of backscattering molecules which return through the aperture due to collision is neglected.

In the case of flow induced by a finite pressure difference between the downstream and upstream reservoirs, or by a temperature difference across a slit or an orifice, the only theoretical results which have appeared to date are Stewart's[6] and Wang and Yu's.[7] Stewart[6] split the flow into two components, the upstream and downstream flows, and applied Willis'[3] iterative method in each direction to obtain two flow rates under the condition of an infinite pressure ratio. The algebraic average of the two values was taken as the net flow rate induced by a pressure difference with a constant temperature across the slit. In this procedure, molecular collisions in the counter-flows which affect the net flow have been completely neglected. By employing Yu's[8] method, Wang and Yu[7] decomposed the distribution function into three parts: two explicit parts, which are singular at the origin, and a remaining part which satisfies an inhomogeneous linear Boltzmann equation. These three parts are presented in multiple integral form, and then asymptotically expanded in powers of the inverse Knudsen number by using the BGK model to obtain the flow rate through a slit under the condition of a finite pressure ratio and temperature difference across the slit. They considered the slit as a line source that absorbs and emits molecules at all velocities. As a source function they used the Maxwellian distribution characterized by the conditions far upstream and downstream. This may not be a good approximation except at extremely high Knudsen numbers. Unfortunately, their first-order correction to the free-molecular flux appears to be a net negative correction, independent of the pressure ratio for the case of constant temperature across the slit, whereas published results obtained either theoretically or experimentally expect a net positive correction to the free-molecular flux.

In the current study, two different approaches, the finite-difference method coupled with the discrete-ordinate method (FDDO)[9–11] and the direct-simulation Monte-Carlo (DSMC) method,[12] are used in the analysis of the flow of a rarefied gas from one reservoir to another through a two-dimensional slit for the cases of vacuum downstream pressure, finite pressure ratios, and isobaric conditions with thermal diffusion. These cases are not well established in spite of the simplicity of the flow field.

In the FDDO analysis, the Boltzmann equation simplified by a model collision integral is solved by means of a finite-difference approximation. Both simple explicit and implicit algorithms are used depending on the characteristics of the velocity space. The velocity space is transformed to a polar-coordinate system and the concept of the discrete-ordinate method is employed to discretize the velocity space. The modified Gauss-Hermite quadrature[11,13] and Simpson's rule are used for the discretized velocity space. A computer code is developed which can be used for any applied pressure and temperature ratio across the slit. In this code, numerical values of flow quantities such as density, velocity, and temperature can be calculated for the entire physical space.

In the DSMC analysis, the variable hard sphere (VHS)[14] model is used as a molecular model and the no time counter (NTC)[15] method is employed as a collision sampling technique.

Problem Statement

Consider the steady flow of a single component, monatomic gas from Reservoir 1 to Reservoir 2 through a two-dimensional slit, as shown in Fig. 1. The equilibrium number densities and pressures of the gas at distances far away from the slit are denoted as n_0 and P_0 in Reservoir 1 and bn_0 and P_b in Reservoir 2. The equilibrium temperature of the gas within Reservoirs 1 and 2 are T_0 and T_b, respectively. The temperature of the slit surface is denoted as T_w. The width of the slit, $2Y_0$, is of the same order as the equilibrium molecular mean free path of the gas in Reservoir 1, so that the flow is not continuum but rarefied. The flow is induced by either a pressure difference or a temperature difference across the slit, or a combination of the two.

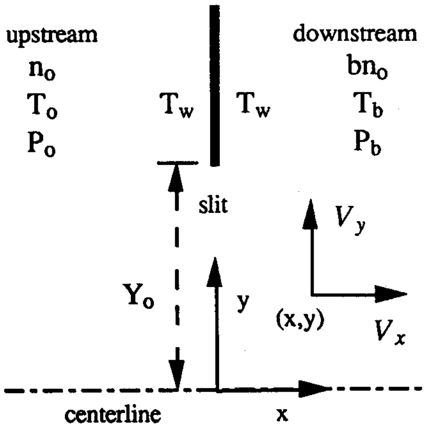

Fig. 1 Coordinate system.

Finite-Difference Method

Governing Equation

We consider the steady-state Boltzmann equation without an external force in a Cartesian coordinate system, as illustrated in Fig. 1

$$V_x \frac{\partial f}{\partial x} + V_y \frac{\partial f}{\partial y} = J \tag{1}$$

where J is the Boltzmann collision integral, which is some functional of f. The moments n, U, and T are given by

$$n = \int f dV; \qquad nU = \int V f dV; \qquad 3nRT = \int C^2 f dV \tag{2}$$

Collision Integral

A solution of the Boltzmann equation is an exceedingly formidable task due to the complicated structure of the collision integral, which contains the details of the molecular interaction. In order to avoid the complex Boltzmann collision integral, several kinetic model equations for monatomic gases such as BGK,[4] Ellipsoidal[16,17] and S model,[18,19] etc., have been proposed. These models retain the fundamental features of molecular collision and average properties of the Boltzmann collision integral and have been extended to gases with internal degrees of freedom[20,21] and to multicomponent gases.[22–24] The collision integral of the kinetic models, J_m, can be represented generally in a form

$$J_m = A_c(F - f) \tag{3}$$

Here A_cF approximates the replenishing collisions, and A_cf the depletion collisions. A collision frequency, A_c, usually is a function of moments and is independent of molecular velocities, whereas F is a function of both moments and molecular velocities.

Modification of the Governing Equation

To reduce the number of independent variables, the following reduced distribution functions are introduced[11]:

$$g(x, y, V_x, V_y) = \int_{-\infty}^{+\infty} f(x, y, V_x, V_y, V_z) dV_z$$

$$h(x, y, V_x, V_y) = \int_{-\infty}^{+\infty} V_z^2 f(x, y, V_x, V_y, V_z) dV_z \tag{4}$$

By integrating out the V_z dependence with the weighting functions 1 and V_z^2, respectively, the equations for the reduced distribution functions with the collision integral of kinetic models of Eq. (3) are obtained from Eq. (1)

$$V_x \frac{\partial g}{\partial x} + V_y \frac{\partial g}{\partial y} + A_c g = A_c G$$

$$V_x \frac{\partial h}{\partial x} + V_y \frac{\partial h}{\partial y} + A_c h = A_c H \qquad (5)$$

where

$$G(x, y, V_x, V_y) = \int_{-\infty}^{+\infty} F dV_z$$

$$H(x, y, V_x, V_y) = \int_{-\infty}^{+\infty} V_z^2 F dV_z$$

Then, using the characteristic length of a flow field d and the most probable thermal speed V_0, the following dimensionless variables are introduced

$$\hat{x} = x/d, \quad \hat{y} = y/d, \quad \hat{n} = n/n_0, \quad \hat{V}_x = V_x/V_0,$$

$$\hat{V}_y = V_y/V_0, \quad \hat{U}_x = U_x/V_0, \quad \hat{U}_y = U_y/V_0,$$

$$\hat{T} = T/T_0, \quad \hat{A}_c = A_c d/V_0, \quad \hat{g} = gV_0^2/n_0,$$

$$\hat{h} = h/n_0, \quad \hat{G} = GV_0^2/n_0, \quad \text{and} \quad \hat{H} = H/n_0 \qquad (6)$$

By introducing a polar coordinate system, which is defined as

$$\hat{V}_x = V \sin\phi$$

$$\hat{V}_y = V \cos\phi$$

$$\phi = \tan^{-1}(\hat{V}_x/\hat{V}_y) \qquad (7)$$

and applying general transformation rules, the governing equations in the new coordinate system (ξ, η) are written as[11]

$$B \frac{\partial \hat{g}}{\partial \eta} + C \frac{\partial \hat{g}}{\partial \xi} + \hat{A}_c \hat{g} = \hat{A}_c \hat{G}$$

$$B \frac{\partial \hat{h}}{\partial \eta} + C \frac{\partial \hat{h}}{\partial \xi} + \hat{A}_c \hat{h} = \hat{A}_c \hat{H} \qquad (8)$$

where

$$B = (V \cos\phi \hat{x}_\xi - V \sin\phi \hat{y}_\xi)/J_t$$

$$C = (V \sin\phi \hat{y}_\eta - V \cos\phi \hat{x}_\eta)/J_t$$

Discrete Ordinate Method

In order to remove the velocity space dependency from the reduced distribution functions, the discrete-ordinate method[9-11] is employed. This method, which consists of replacing the integration over velocity space of the distribution functions by appropriate integration formulas, requires the values of the distribution functions only at certain discrete speeds and velocity angles. The choice of the discrete values of V and ϕ are dictated by the consideration that our final interest is not in the distribution functions themselves but in the moments. Hence, the macroscopic moments given by integrals over the molecular velocity space can be calculated by proper integration formulas. Applying the method, the following quadratures are substituted for the integrals in Eqs. (2)

$$\hat{n} = \sum_\delta \int_0^{2\pi} P_\delta \hat{g}_\delta d\phi$$

$$\hat{n}\hat{U}_x = \sum_\delta \int_0^{2\pi} P_\delta V_\delta \sin\phi \hat{g}_\delta d\phi$$

$$\hat{n}\hat{U}_y = \sum_\delta \int_0^{2\pi} P_\delta V_\delta \cos\phi \hat{g}_\delta d\phi$$

$$\frac{3}{2}\hat{n}\hat{T} = \sum_\delta \int_0^{2\pi} P_\delta(\hat{h}_\delta + V_\delta^2 \hat{g}_\delta) d\phi - \hat{n}(\hat{U}_x^2 + \hat{U}_y^2) \qquad (9)$$

where $\hat{g}_\delta$ and $\hat{h}_\delta$ denote $\hat{g}(\xi, \eta, V_\delta, \phi)$, and $\hat{h}(\xi, \eta, V_\delta, \phi)$, respectively. Thus, instead of solving the equations for a function of space and molecular velocity, the equations are transformed to partial differential equations, which are continuous in space but are point functions in molecular speed, V, and velocity angle, ϕ, as follows

$$B \frac{\partial \hat{g}_\delta}{\partial \eta} + C \frac{\partial \hat{g}_\delta}{\partial \xi} + \hat{A}_c \hat{g}_\delta = \hat{A}_c \hat{G}_\delta$$

$$B \frac{\partial \hat{h}_\delta}{\partial \eta} + C \frac{\partial \hat{h}_\delta}{\partial \xi} + \hat{A}_c \hat{h}_\delta = \hat{A}_c \hat{H}_\delta \qquad (10)$$

where

$$B = (V_\delta \cos\phi \hat{x}_\xi - V_\delta \sin\phi \hat{y}_\xi)/J_t$$

$$C = (V_\delta \sin\phi \hat{y}_\eta - V_\delta \cos\phi \hat{x}_\eta)/J_t$$

$$\hat{G}_\delta = \frac{V_0^2}{n_0} \int_{-\infty}^{\infty} f(\xi, \eta, V_\delta, \phi, V_z) dV_z$$

$$\hat{H}_\delta = \frac{1}{n_0} \int_{-\infty}^{\infty} V_z^2 f(\xi, \eta, V_\delta, \phi, V_z) dV_z$$

Finite-Difference Algorithm

Eqs. (10) are solved by means of finite-difference approximations in physical space. To reduce CPU time, a simple explicit scheme is used for ξ.

$$\frac{\partial \hat{g}_\delta}{\partial \xi} \cong \frac{\hat{g}_\delta(\xi, \eta) - \hat{g}_\delta(\xi - js\Delta\xi, \eta)}{js\Delta\xi} \qquad (11)$$

where

$$js = \text{sign}[(V_\delta \sin\phi \hat{y}_\eta - V_\delta \cos\phi \hat{x}_\eta)/J_t]$$

The following finite-difference schemes are used for η, which depend on the characteristics of physical and velocity space

$$\frac{\partial \hat{g}_\delta}{\partial \eta} \cong \frac{\hat{g}_\delta(\xi, \eta) - \hat{g}_\delta(\xi, \eta - is\Delta\eta)}{is\Delta\eta} \qquad (12)$$

$$\frac{\partial \hat{g}_\delta}{\partial \eta} \cong \frac{\hat{g}_\delta(\xi, \eta + \Delta\eta) - (\hat{g}_\delta(\xi, \eta - \Delta\eta)}{2\Delta\eta} \qquad (13)$$

where

$$is = \text{sign}[(V_\delta \cos\phi \hat{x}_\xi - V_\delta \sin\phi \hat{y}_\xi)/J_t]$$

Taking equivalent finite-difference schemes for $\hat{h}_\delta$, the system of nonlinear algebraic equations are to be solved by the method of successive approximations. In the iterative procedure, only the values of $\hat{A}_c$, $\hat{G}_\delta$, and $\hat{H}_\delta$ have to be determined from moments of the previous iteration, and the values of distribution functions do not need to be stored. Convergence is assumed to have occurred when the differences of the moments of two successive iteration steps are kept within the bound of prescribed tolerance at every spatial grid point.

By checking consistency and stability according to the equivalence theorem of Lax,[25] the convergence of the finite-difference approximations is ensured.[11] A Von Neumann analysis made for the linearized form of the finite-difference approximations[11] shows that the finite-difference approximations are unconditionally stable regardless of computational grid sizes by choosing appropriate marching directions following the motion of each molecule both in physical and velocity space.

Model Equation

For the collision integral, the BGK[4] model is chosen for the sake of simplicity. In this model, F is given by the Maxwell-Boltzmann distribution

$$F = n(2\pi RT)^{-3/2} \exp(-C^2/2RT) \tag{14}$$

The collision frequency A_c is taken to be of the form[26]

$$A_c = mnRT/\mu \tag{15}$$

The viscosity, μ, is assumed to have a temperature dependency[26]

$$\frac{\mu}{\mu_0} = \left(\frac{T}{T_0}\right)^s \tag{16}$$

where s is a constant for a given gas. The viscosity at the upstream reservoir condition, μ_0, is related to the upstream mean free path, λ_0, by the relation

$$\lambda_0 = \frac{16}{5} \frac{\mu_0}{mn_0(2\pi RT_0)^{1/2}} \tag{17}$$

The characteristic length of the flow field is chosen as the slit half-width. Combining Eqs. (14) to (17), we obtain

$$\hat{G} = \frac{\hat{n}}{\pi \hat{T}} \exp(-[(V\cos\phi - \hat{U}_y)^2 + (V\sin\phi - \hat{U}_x)^2]/\hat{T} \tag{18}$$

$$\hat{H} = \frac{1}{2}\hat{T}\hat{G}, \qquad \hat{A}_c = \frac{4}{5\pi^{1/2}} \frac{\hat{n}\hat{T}^{1-s}}{Kn} \tag{19}$$

$$Kn = \lambda_0/2Y_0 \tag{20}$$

where Kn is the Knudsen number at the upstream reservoir condition based on the slit width.

Boundary Conditions

The following boundary conditions are used for the calculation: 1) At infinity in the upstream reservoir, there is an equilibrium distribution with prescribed reservoir conditions: $\hat{n}_0$ and $\hat{T}_0$

$$\hat{g} = \frac{\hat{n}_0}{\pi \hat{T}_0} \exp(-V^2/\hat{T}_0$$

$$\hat{h} = \frac{1}{2}\hat{T}_0 \hat{g} \tag{21}$$

2) Similarly, in the downstream reservoir

$$\hat{g} = \frac{b\hat{n}_0}{\pi \hat{T}_b} \exp(-V^2/\hat{T}_b)$$

$$\hat{h} = \frac{1}{2}\hat{T}_b \hat{g} \tag{22}$$

3) In order to specify the interaction of the molecules with the surface, diffuse reflection is assumed, i.e., molecules that strike the surface are subsequently emitted with a Maxwell distribution characterized by the surface temperature $\hat{T}_w$:

$$\hat{g} = \frac{\hat{n}_w}{\pi \hat{T}_w} \exp(-V^2/\hat{T}_w), \quad \text{for} \quad (\boldsymbol{V}\cdot\boldsymbol{n}) < 0$$

$$\hat{h} = \frac{1}{2}\hat{T}_w \hat{g}, \quad \text{for} \quad (\boldsymbol{V}\cdot\boldsymbol{n}) < 0 \tag{23}$$

The wall number flux $\hat{n}_w$ is not known a priori and may be determined by applying the condition of no net flux normal to the surface

$$\hat{n}_w = -2(\pi/\hat{T}_w)^{1/2} \int_0^\infty \int_\phi (\boldsymbol{V}\cdot\boldsymbol{n})\hat{g} V dV d\phi, \text{ for } \quad (\boldsymbol{V}\cdot\boldsymbol{n}) > 0 \tag{24}$$

4) Along the centerline, symmetric boundary conditions are used

$$\hat{g}(\xi, \eta = 0, \phi) = \hat{g}(\xi, \eta = 0, \pi - \phi)$$

$$\hat{h}(\xi, \eta = 0, \phi) = \hat{h}(\xi, \eta = 0, \pi - \phi) \tag{25}$$

Numerical Procedure

The finite-difference approximations of Eqs. (10) are solved by the method of successive approximations. In each iteration step, the calculation starts at the point ($\eta = \eta_\infty - \Delta\eta$, $\xi = \xi_\infty + \Delta\xi$) for a chosen discrete-ordinate V_δ. For this discrete-ordinate, the values of the distribution functions are then determined at all (ξ, η) grid points for the quadrant of velocity angle $\pi/2 \leq \phi \leq \pi$. Then, applying the symmetric condition Eq. (25), the values of the distribution functions at the centerline are determined for the quadrant of velocity angle $\pi/2 \geq \phi \geq 0$ and calculated at all (ξ, η) grid points starting from the point ($\eta = \Delta\eta$, $\xi = \xi_{-\infty} + \Delta\xi$). An analogous procedure is carried out for the quadrant of velocity angle $-\pi \leq \phi \leq -\pi/2$ and $-\pi/2 \leq \phi \leq 0$ starting from the point ($\eta = \eta_\infty - \Delta\eta$, $\xi = \xi_{-\infty} - \Delta\xi$) and ($\eta = \Delta\eta$, $\xi = \xi_{-\infty} - \Delta\xi$), respectively. After this procedure is repeated for all discrete-ordinates V_δ for both $\hat{g}_\delta$ and $\hat{h}_\delta$, the wall number flux $\hat{n}_w$ and the moments may be calculated by means of the quadrature formula, Eq. (9), with a proper integration method over the angle. The iterative procedure is stopped when the difference of all moments between two iterative steps $I + 1$ and I, $|(M^{I+1} - M^I)/M^I|$ are less than 10^{-3} for all spatial grid points. As a proper quadrature formula, the modified Gauss-Hermite half range quadrature for integrals of the form[11,13]

$$\int_0^\infty \exp(-V^2)V^j Q(V) dV = \sum_{\delta=1}^{N} P_\delta Q(V_\delta) \tag{26}$$

is used. The exponent j and the order of the quadrature N are chosen to be 1 and 8, respectively. Simpson's 3/8th rule with $\Delta\phi = 4.5$ deg is used for the integration over the angle ϕ. The (η, ξ) plane was covered by 51 × 21 grid points for the upstream reservoir and 51 × 31 for the downstream reservoirs. The exponent of the viscosity-temperature relation in Eq. (16), s, was that for Argon, 0.811. The surface temperature was chosen to be the same as that in the far upstream reservoir.

Direct-Simulation Monte-Carlo Method

In the present study, the NTC method developed by Bird[15] is used as a sampling technique. In the NTC method, the number of pairs to be sampled, N_S, is given by

$$N_S = N_m n(\sigma_T C_r)_{\max} \Delta t/2 \tag{27}$$

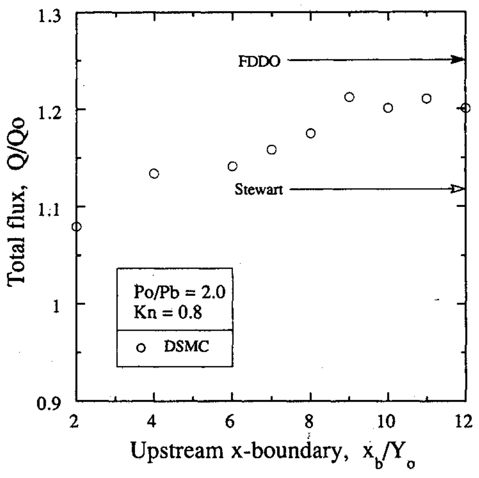

Fig. 2 Effect of the location of upstream x-boundary on the total flux.

and the collision probability for each selection is

$$(\sigma_T C_r)/(\sigma_T C_r)_{\max} \tag{28}$$

For the molecular model, the VHS model developed by Bird[14] is employed. In the VHS model, the collision cross section is given by

$$\sigma_T \alpha C_r^{-2w} \tag{29}$$

where w is related to the viscosity-temperature exponent, s, by

$$s = w + 0.5 \tag{30}$$

In DSMC calculations, the best results may be obtained for the largest possible number of simulated molecules, for the cell size as small as possible in comparison with the mean free path, and for discrete time step Δt as small as possible in comparison with the mean collision time. In most of the calculations, the cell size, Δx and Δy, was less than 0.2 and the time step was less than 0.04. Here the cell size is measured in units of the upstream mean free path, λ_0, and Δt in units of λ_0/V_0.

Another important factor that should be considered will be the size of the simulated space. The distance from the slit to the boundaries was increased until a further increase in that direction did not result in any noticeable change in the total flux through the slit. It was found that the location of the upstream x-boundary, which is parallel to the y axis, had the most significant effect on the result. Figure 2 shows the effect of the upstream x-boundary in the case of the finite downstream pressure of $P_0/P_b = 2.0$ at Knudsen number 0.8. In the figure, x_b is the distance from the slit to the boundary. In most of the calculations, the x-boundary was chosen to be $10Y_0$ both upstream and downstream, and the y-boundary $5Y_0$ both upstream and downstream.

In most of the calculations, the average number of molecules per cell was kept around 20 with at least 10 molecules in the cells at far downstream. Sampling interval was $5\Delta t$ and average sample size per cell was around 50,000. The exponent of the VHS model, w, was that for Argon, 0.311.

Results and Discussion

For the case of free-molecular flow, there are no collisions between molecules and molecules move until they reach the surface of a body. Thus, at any point in the physical space, the velocity space can be divided into two regions: one for molecules coming from the reservoirs and the other for molecules emitted from the surface. Since exact values of the distribution function can be obtained for each of these regions, theoretical values of moments for free-molecular flow conditions may be obtained by integrating these distribution functions. If $T_0 = T_b = T_w$, the following analytical equations for the theoretical free-molecular macroscopic moments at the centerline can be obtained

$$\hat{n} = 0.5(1 + b) - \frac{\hat{x}}{|\hat{x}|}(1 - b)$$
$$\left[0.5 - \frac{1}{\pi}\sin^{-1}\left(\frac{1}{\sqrt{1 + \hat{x}^2}}\right)\right] \tag{31}$$

$$\hat{U}_x = \frac{1 - b}{2\sqrt{\pi\hat{n}}\sqrt{1 + \hat{x}^2}} \tag{32}$$

$$\hat{T} = 1 - \frac{2}{3}\hat{U}_x^2 \tag{33}$$

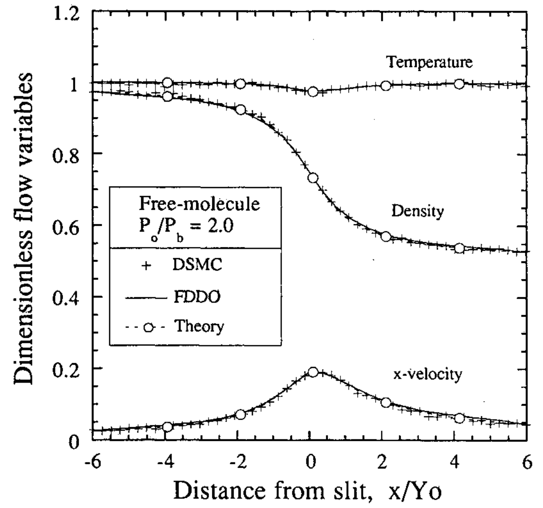

Fig. 3 Free-molecular macroscopic flow variables along the centerline in the case of a finite downstream pressure.

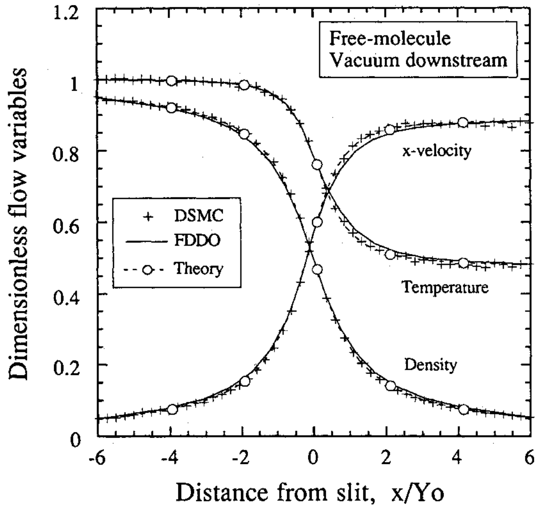

Fig. 4 Free-molecular macroscopic flow variables along the centerline in the case of a vacuum downstream.

In Figs. 3 and 4, the free-molecular macroscopic moments along the centerline for the cases of a finite downstream pressure of $P_0/P_b = 2$ and a vacuum downstream are compared with the theoretical solutions, respectively. The results of both the FDDO and the DSMC methods show good agreement with the theoretical solutions.

In Fig. 5, the total flux as a function of Knudsen number for the case of a vacuum in the downstream reservoir is compared with Willis'[5] results obtained by the first iterative method with the linearized BGK model and with Wang and Yu's[7] results by the first-order correction method with a linearized BGK model, as well as with the results of the DSMC method. Here the dimensionless total flux Q/Q_0 is defined as

$$\frac{Q}{Q_0} = \frac{\int_A Q_x dA}{\int_A Q_{x0} dA} \tag{34}$$

where the integration is performed over the aperture area A and the fluxes Q_x and Q_{x0} are defined as

$$Q_x = \int_0^\infty \int_0^{2\pi} \hat{g} V^2 \sin\phi dV d\phi \tag{35}$$

$$Q_{x0} = Q_{xu} + Q_{xb} \tag{36}$$

$$Q_{xu} = \int_0^\infty \int_0^\pi \frac{\hat{n}_0}{\pi \hat{T}_0} \exp(-V^2/\hat{T}_0) V^2 \sin\phi dV d\phi \tag{37}$$

$$Q_{xb} = \int_0^\infty \int_\pi^{2\pi} \frac{b\hat{n}_0}{\pi \hat{T}_b} \exp(-V^2/\hat{T}_b) V^2 \sin\phi dV d\phi \tag{38}$$

Except for Wang and Yu's[7] results that show negative corrections to the free-molecular flux, the results from other methods show positive correction. Willis'[5] results show fairly good agreement at large Knudsen numbers. However, Willis' first iterate method severely underestimated the total flux at small Knudsen numbers compared to the results of the other methods. This is because he neglected the effect of backscattering molecules, which return through the aperture due to collision. The results of the DSMC method show good agreement with those of the FDDO method. Two kinds of model equations, the BGK and the S model, are employed in the FDDO method. There were not significant differences between the results of BGK model[4] and the S model[18,19] in the FDDO method. In the S model, the quantity F in Eq. (3) is given by

$$F = F^0 \left[1 + \frac{1 - Pr}{5} \frac{2(C \cdot q)}{PRT} \left(\frac{C^2}{2RT} - \frac{5}{2} \right) \right] \tag{39}$$

$$F^0 = \frac{n}{(2\pi RT)^{3/2}} \exp(-C^2/2RT) \tag{40}$$

$$q = \frac{m}{2} \int C^2 C f dV \tag{41}$$

In the computation, the S model needs more CPU time and storage than the BGK model because the quantity in the bracket of Eq. (39) should be calculated at every grid point for each discrete speed and velocity angle during iteration.

Comparison is shown in Fig. 6 of the predicted exit plane fluxes in a slit with a vacuum downstream for the case of $Kn = 0.2$. Here the dimensionless flux Q_x/Q_{x0} is given by

$$\frac{Q_x}{Q_{x0}} = \frac{2\sqrt{\pi}}{1 - b\sqrt{\hat{T}_b}} \int_0^\infty \int_0^{2\pi} \hat{g} V^2 \sin\phi dV d\phi \tag{42}$$

Willis' method severely underestimates the flux, which was the case with the total flux. The results of the FDDO method show good agreement with those of the DSMC method.

In Fig. 7, the predicted density, temperature, and x-velocity distributions along the centerline at Knudsen number 0.2 in the case of vacuum downstream are compared, respectively. The results of both the FDDO and the DSMC methods show good agreement. In the case of a vacuum downstream, the temperature decreases rapidly across the slit and then gradually approaches a certain limit in the downstream, i.e., the temperature freezes. As the gas expands in both the parallel and perpendicular directions, the temperature falls because of the geometric expansion. As the gas further expands, the perpendicular temperature still decreases from geometric expansion. Collisional cooling of parallel temperature, however, stops, i.e., freezes. Hence, far downstream along the centerline, the perpendicular temperature decreases to zero and the

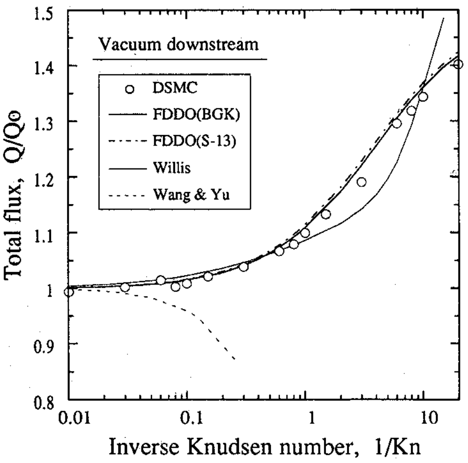

Fig. 5 Total flux through a slit in the case of a vacuum downstream.

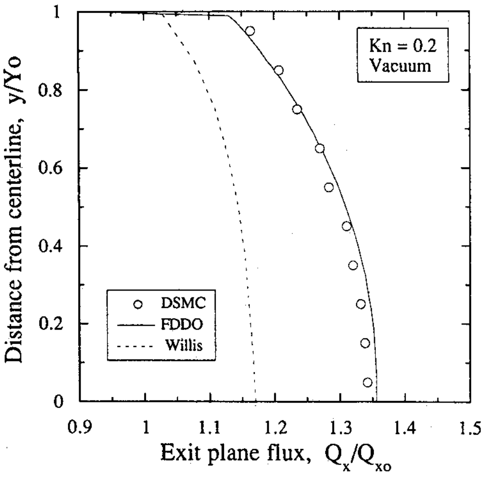

Fig. 6 Exit plane flux distribution through a slit at $Kn = 0.2$ in the case of a vacuum downstream.

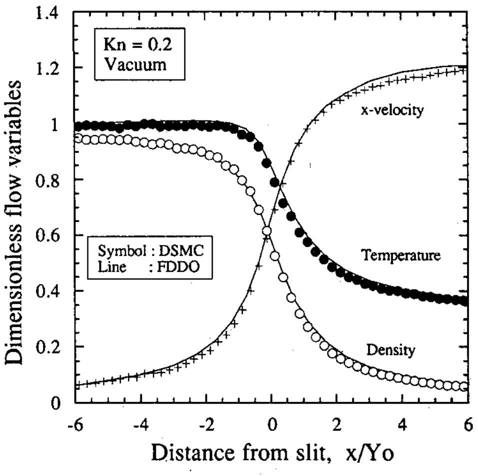

Fig. 7 Distribution of macroscopic flow variables along the centerline of a slit at $Kn = 0.2$ in the case of a vacuum downstream.

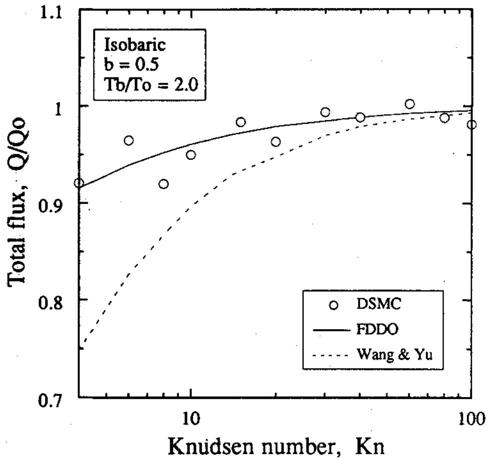

Fig. 8 Total flux through a slit in the case of an isobaric condition across a slit.

total temperature remains constant. The velocity along the centerline of a slit with a vacuum downstream increases according to collision dominated expansion until reaching the collisionless stage. The increase of velocity, then, stops, i.e., the velocity freezes.

Comparison is shown in Fig. 8 of the predicted total flux as a function of Knudsen numbers with the ratio of the downstream to the upstream temperature, $T_b/T_0 = 2.0$, and isobaric condition through a slit. In this case, the flow is induced by both the temperature and density differences through the slit. The solid line shows the result of the FDDO method and the dotted line those of Wang and Yu.[7] The results of both the FDDO and the DSMC methods show good agreement. Wang and Yu's first-order correction method with the linearized BGK model severely underestimates the total flux in case of an isobaric condition through the slit, which was also the situation in the vacuum downstream case.

To obtain a steady-state solution, the FDDO method requires an iterative procedure and the DSMC method needs many time steps until reaching the large time solution for an unsteady flow. In the FDDO method, to reduce CPU time, macroscopic flow variables from a previous solution are effectively used as starting values for a solution at a different Knudsen number. By this procedure, solutions for a wide range of discrete Knudsen numbers can be obtained in a relatively short CPU time per solution. The required CPU time for a solution at a specific Knudsen number greatly depends on the starting value. Another factor on the CPU time requirement would be the effectivenss of coding. Thus, it is difficult to compare the CPU time requirements for both the FDDO and the DSMC methods. A rough comparison, however, could be made based on the calculations selected in the present study.

For free-molecular solutions, on an NAS/9080, the FDDO method required only one iteration of about 3 min and the DSMC methods about 120 min for the sample size used in the present study. At high Knudsen numbers, $Kn > 1$, the FDDO method required 9–15 min (3–5 iterations) using a solution at a Knudsen number about two times larger as an initial guess, and the DSMC methods 120–160 min. At small Knudsen numbers, $1 > Kn > 0.05$, the FDDO method required 15–30 min (5–10 iterations), and the DSMC methods 160–240 min. The CPU storage requirement for the FDDO and the DSMC methods were about 0.5 and 4.0 mega words, respectively.

Conclusions

Two different approaches, the finite-difference method coupled with the discrete-ordinate method (FDDO), and the direct-stimulation Monte-Carlo (DSMC) method, are used in the analysis of the flow of a rarefied gas from one reservoir to another through a two-dimensional slit. The cases considered are for vacuum downstream pressure, finite pressure ratios, and isobaric conditions with thermal diffusion. The FDDO method has been shown to be a practical method for treating the flow of rarefied gases through a slit. In the DSMC analysis, the variable hard sphere (VHS) model is used as a molecular model and the no time counter (NTC) method is employed as a collision sampling.

The results of both the FDDO and the DSMC methods showed good agreement. The FDDO method required less CPU time than the DSMC method by factors of 10 to 40 depending on the degree of rarefaction for the cases selected in the present study. Also, the FDDO method required less CPU storage than the DSMC method by a factor of 4.

The FDDO method may be easily applied to rarefied gas flows with complex geometries such as flow through nozzles[9,11] or over submerged bodies.[10,11] Also, the extension of the FDDO method to a rarefied gas flow with internal degrees of freedom or multicomponent gases can be easily made by employing the collision integrals for such gases[21–26] and the distribution functions for each species.

Acknowledgment

This work was sponsored in part by the NASA Lewis Research Center, Cleveland, Ohio, under Grant NAG 3-577. Earl Morren is the grant director.

References

[1] Liepmann, H. W., "Gaskinetics and Gasdynamics of Orifice Flow," *Journal of Fluid Mechanics*, Vol. 10, Part 1, 1961, pp. 65–79.

[2] Narasimha, R., "Orifice Flow at High Knudsen Numbers," *Journal of Fluid Mechanics*, Vol. 10, Part 3, 1961, pp. 371–384.

[3] Willis, D. R., *Princeton Univ. Aeronaut. Eng. Rep. No. 442*, 1958, p. 371.

[4] Bhatnagar, P. L., Gross, E. P., and Krook, M., "A Model for Collision Processes in Gases. I. Small Amplitude Processes in Charged and Neutral One-Component Systems," *Physical Review*, Vol. 94, No. 3, 1954, pp. 511–525.

[5] Willis, D. R., "Mass Flow Through a Circular Orifice and a Two-Dimensional Slit at High Knudsen Numbers," *Journal of Fluid Mechanics*, Vol. 21, Part 1, 1965, pp. 21–31.

[6] Stewart, J. D., "Mass Flow Rate for Nearly-Free-Molecular Slit Flow," *Journal of Fluid Mechanics*, Vol. 35, Part 3, 1969, pp. 599–608.

[7] Wang, P. Y., and Yu, E. Y., "Nearly Free-Molecular Slit Flow at Finite Pressure and Temperature Ratios," *Journal of Fluid Mechanics*, Vol. 50, Part 3, 1971, pp. 565–577.

[8] Wang, P. Y., and Yu, E. Y., "Fundamental Solution of the Linear Boltzmann Equation," *Physics of Fluids*, Vol. 10, No. 11, 1967, pp. 2466–2474.

[9] Chung, C. H., De Witt, K. J., Jeng, D. R., and Keith, T. G. Jr., "Rarefied Gas Flow Through Two-Dimensional Nozzles," AIAA Paper 89-2893, July 1989.

[10] Chung, C. H., Jeng, D. R., De Witt, K. J., and Keith, T. G. Jr., "Flow of Rarefied Gases over Two-Dimensional Bodies," *Proceedings of AIAA 9th Computational Fluid Dynamics Conference*, Buffalo, New York, June 1989, pp. 389–399.

[11] Chung, C. H., Ph.D. Dissertation, University of Toledo, 1990.

[12] Bird, G. A., *Molecular Gas Dynamics*, Oxford University Press, London, 1976.

[13] Shizgal, B., "A Gaussian Quadrature Procedure for Use in the Solution of the Boltzmann Equation and Related Problems," *Journal of Computational Physics*, Vol. 41, No. 2, 1981, pp. 309–328.

[14] Bird, G. A., "Monte Carlo Simulation in an Engineering Context," *Progress in Astronautics and Aeronautics: Rarefield Gas Dynamics*, edited by S. S. Fisher, Vol. 74, AIAA, New York, 1981, pp. 239–255.

[15] Bird, G. A., "The Perception of Numerical Methods in Rarefied Gas Dynamics," *Progress in Astronautics and Aeronautics: Rarefied Gas Dynamics*, edited by E. P. Muntz, D. P. Weaver, and D. H. Campbell, Vol. 118, 1989, pp. 211–226.

[16] Holway, L. H. Jr., "New Statistical Model for Kinetic Theory: Method of Construction," *Physics of Fluids*, Vol. 9, No. 9, 1966, pp. 1658–1673.

[17] Cercignani, C., and Tironi, G., "Some Application of a Linear-

ized Kinetic Model with Correct Prandtl Number," *Nuovo Cimento*, Vol. 43B, No. 1, 1966, pp. 64–78.

[18] Shakhov, E. M., "Generalization of The Krook Kinetic Relaxation Equation," *Fluid Dynamics*, Vol. 3, No. 1, 1968, pp. 95–97.

[19] Abe, T., and Oguchi, H., "A Hierarchy Kinetic Model and Its Applications," *Progress in Astronautics and Aeronautics*, edited by J. L. Potter, Vol. 51, AIAA New York, 1977, pp. 781–794.

[20] Morse, T. F., "Kinetic Model of Gases with Internal Degrees of Freedom," *Physics of Fluids*, Vol. 7, No. 2, 1964, pp. 159–169.

[21] Rykov, V. A., "A Model Kinetic Equation for a Gas with Rotational Degrees of Freedom," *Fluid Dynamics*, Vol. 10, No. 6, 1975, pp. 959–966.

[22] Sirovich, L., "Kinetic Modeling of Gas Mixtures," *Physics of Fluids*, Vol. 5, No. 8, 1962, pp. 908–924.

[23] Hamel, B. B., "Kinetic Model for Binary Gas Mixtures," *Physics of Fluids*, Vol. 8, No. 3, 1965, pp. 418–425.

[24] Garzó, V., Santos, A., and Brey, J. J., "Kinetic Model for Gases with Internal Degrees of Freedom," *Physics of Fluids A*, Vol. 1, No. 2, 1989, pp. 380–383.

[25] Anderson, D. A., Tannehill, J. C., and Pletcher, R. H., *Computational Fluid Mechanics and Heat Transfer*, McGraw-Hill, New York, 1984.

[26] Chapman, S., and Cowling, T. G., *The Mathematical Theory of Non-Uniform Gases*, Cambridge University Press, London, 1958.

Recommended Reading from the AIAA
Progress in Astronautics and Aeronautics Series . . . AIAA

Dynamics of Explosions
and
Dynamics of Reactive Systems, I and II

J. R. Bowen, J. C. Leyer, and R. I. Soloukhin, editors

Companion volumes, *Dynamics of Explosions and Dynamics of Reactive Systems, I and II*, cover new findings in the gasdynamics of flows associated with exothermic processing—the essential feature of detonation waves—and other, associated phenomena.

Dynamics of Explosions (volume 106) primarily concerns the interrelationship between the rate processes of energy deposition in a compressible medium and the concurrent nonsteady flow as it typically occurs in explosion phenomena. *Dynamics of Reactive Systems* (Volume 105, parts I and II) spans a broader area, encompassing the processes coupling the dynamics of fluid flow and molecular transformations in reactive media, occurring in any combustion system. The two volumes, in addition to embracing the usual topics of explosions, detonations, shock phenomena, and reactive flow, treat gasdynamic aspects of nonsteady flow in combustion, and the effects of turbulence and diagnostic techniques used to study combustion phenomena.

Dynamics of Explosions
1986 664 pp. illus., Hardback
ISBN 0-930403-15-0
AIAA Members $54.95
Nonmembers $92.95
Order Number V-106

Dynamics of Reactive Systems I and II
1986 900 pp. (2 vols.), illus. Hardback
ISBN 0-930403-14-2
AIAA Members $86.95
Nonmembers $135.00
Order Number V-105

***TO ORDER:* Write, Phone or FAX:** American Institute of Aeronautics and Astronautics, c/o TASCO,
9 Jay Gould Ct., P.O. Box 753, Waldorf, MD 20604 Phone (301) 645-5643, Dept. 415 FAX (301) 843-0159

Sales Tax: CA residents, 7%; DC, 6%. Add $4.75 for shipping and handling of 1 to 4 books (Call for rates on higher quantities). Orders under $50.00 must be prepaid. Foreign orders must be prepaid. Please allow 4 weeks for delivery. Prices are subject to change without notice. Returns will be accepted within 15 days.